Article

Interfaces design in lightweight SiC/$TiSi_2$ composites fabricated by reactive infiltration process: Interaction phenomena between liquid Si-rich Si-Ti alloys and glassy carbon

Donatella Giuranno[1]*, Sofia Gambaro[1], Grzegorz Bruzda[2], Rafal Nowak[2], Wojciech Polkowski[2], Natalia Sobczak[2, 3], Simona Delsante[4], Rada Novakovic[1]

[1]Institute of Condensed Matter Chemistry and Technologies for Energy (ICMATE), National Research Council of Italy (CNR),Via De Marini 6, Genoa, 16149, Italy. donatella.giuranno@ge.icmate.cnr.it; sofia.gambaro@ge.icmate.cnr.it; rada.novakovic@ge.icmate.cnr.it
[2]Lukasiewicz Research Network-Foundry Research Institute, Zakopiańska 73 Str., 30-418 Krakow, Poland. grzegorz.bruzda@kit.lukasiewicz.gov.pl; rafal.nowak@kit.lukasiewicz.gov.pl wojciech.polkowski@ kit.lukasiewicz.gov.pl
[3]Institute of Metallurgy and Materials Science, Polish Academy of Sciences (IMMS-PAS), 25 Reymonta Str., 30-059 Krakow, Poland. n.sobczak@imim.pl
[4]Department of Chemistry and Industrial Chemistry, Genoa University and Genoa Research Unit of INSTM, Via Dodecaneso 31, 16146, Genoa, Italy. simona.delsante@unige.it
* Correspondence: donatella.giuranno@ge.icmate.cnr.it

Abstract:

To design properly and optimize liquid-assisted processes such as reactive infiltration for fabricating lightweight and corrosion resistant SiC/$TiSi_2$ composites, the interfacial phenomena taking place when liquid Si-rich Si-Ti alloys are in contact with glassy carbon (GC) were investigated for the first time by wetting tests performed by both the sessile and pendant drop methods at T = 1450°C. Specifically, two different Si-rich Si-Ti alloys were selected, and the obtained results in terms of contact angle values, spreading kinetics, reactivity, and developed interface microstructures were compared with experimental observations previously obtained for the liquid Si-rich Si-Ti eutectics processed under the same operating conditions. The increase of the Si content did not affect the final contact angle values. Contrarily, the final developed microstructure at the interface as well as the spreading kinetics were observed as weakly dependent on the composition. From the practical point of view, Si-Ti alloy compositions with a Si-content falling in the simple eutectic region of the phase diagram might be potentially used as infiltrant materials of C- and SiC-based composites.

Keywords: MMCs; CMCs, Aerospace; Wetting at high temperature; Ti-Silicides.

1. Introduction

Industrial sectors belonging to the light-weight transportation and aerospace continue to base their research and innovation plans on three fundamental pillars: lighter weight, increased strengths and enhanced heat and corrosion resistances [1]. The motivations behind lie in reducing the air and spacecraft manufacture costs, improving fuel economy through efficiency and light-weighting and making air and space travels more cost-effective and safer modes of transportation [2].

In this context, the materials gaining the highest interest are basically: metal and ceramic matrix composites (MMCs and CMCs) reinforced by high strength continuous ceramic fibers, freshly machinable metals, and materials of new concept, such as bulk metallic glasses (BMGs) and high entropy alloys (HEAs) as ideal replacements for the less "virtue" and more traditional structural materials (i.e. Ni-based superalloys, steels, etc.) [3-6].

For aerospace and light weight transportation applications, today the most extensively studied CMCs are reinforced by C- and SiC fibers (C_f and SiC_f, respectively), namely C_f/C, C_f/SiC, SiC_f/SiC and C_f/C-SiC composites, as well as SiC_P (SiC particles as reinforcement) [1, 3, 4, 7-12].
Despite the manufacturing processes of fibers and reinforcements have reached a high level of reproducibility, their use is limited by the costs and technological problems encountered in producing successfully large and complex CMCs shapes. By the way, key steps are CMCs assembling and their integration/joining with dissimilar materials, i.e., metals, ceramics or other composites, as well as fibers degradation during the fabrication processes and in service, mainly at high temperature. Indeed, C_f and SiC_f show the tendency to be oxidized and degraded (i.e. by releasing $CO_{(g)}$ and $SiO_{(g)}$) if processed at temperature above 400°C and 1300°C under oxidizing atmospheres, respectively [13, 14].

Several papers available in literature point out metal silicides as promising densifiers or filler phases for CMCs for improving thermal barriers [8, 15], as structural materials and components for assembling re-entry space vehicles [10, 16] and fission/fusion nuclear reactors [17- 19]. It is for their peculiarities, such as chemical inertness, improved electrical and thermal stability, self-protection and self-healing features due to their excellent oxidation resistance, mainly at high temperatures and, for some of the applications mentioned above, for their limited weight, as in the case of Ti-silicides.
To succeed in the fabrication/joining of such composites, the spontaneous/pressure-less infiltration of liquid Ti- or Si-based alloys can be considered as a costless alternative than conventional sintering processes. In addition, if compared with sintering techniques, the Si-based alloys infiltration into C- and SiC-based porous materials show significant benefits. It is a classical liquid-assisted process based on the Reaction Bonded/formed Silicon Carbide mechanisms (e.g. RBSC/RFSC), well-known evolving at lower processing parameters (i.e. temperature, pressure and time) with nearly-net shape fabrication capabilities [20, 21]. On the other hand, for liquid-assisted processes applied for densifying/joining CMCs matrixes, the pivotal issue is to preserve the starting fibers microstructure, meaning their thermo-mechanical response. In other words, it lies in the successful control of the interaction phenomena taking place at the metal/fiber interfaces and to successfully achieve the reliability, key requirements include a chemical-physical compatibility between the liquid metal phase and fibers, in terms of good wetting/adhesion but limited reaction phenomena, comparable thermal expansion coefficient (CTE), etc. In addition, to avoid the fiber degradation, a suitable set of process parameters needs to be defined, such as a reduced oxygen content inside the working atmosphere and a temperature ≤ 1450°C.

A few previous attempts to use Si-rich Si-Ti alloys (hearafter Si-Ti alloys), including the liquid $TiSi_2$ and Si-rich eutectic (i.e. Si-16at%Ti) alloys, as brazers and densifying materials for CMC, are available literature [18-29], even provided by the authors [30]. Specifically, the use of Si-Ti eutectics for joining monolithic SiC and C_f/C, C_f/C-SiC and SiC_f/SiC composites at T ≤1420°C without any or negligible degradation of the fiber/matrix interfaces in the composite materials are reported [23, 26, 30]. Moreover, the joints produced showed absence of defects or debonding at the interface and a well adherent layer appeared at the metal matrix/fiber interphase. Specifically, as reported in [26, 30], a Si–$TiSi_2$ eutectic microstructure constituted the brazing seam, as driven by the cooling process, combined with the appearance of a dense SiC layer well adherent to C and SiC fibers and an overall improvement of the mechanical properties of the joints was documented.
C_f/C composites were brazed successfully at T ≥ 1490°C using directly $TiSi_2$ as filler alloy by Dadras et al. [31] and a maximum shear strength of 34.4 MPa at T = 1164 °C was measured at the joint, confirming the fair capabilities of using intermetallic alloys as CMC fillers/brazers for applications at high temperatures. By the way, as the authors highlighted, at the bond interlayer of samples joined with $TiSi_2$ interlayers, TiC and SiC were revealed together with the unreacted $TiSi_2$, most probably due to the uncompleted reaction between $TiSi_2$ and C.

Aiming to optimize melt infiltration process, the higher melting point [32] and less fluidity [33] of Ti silicide respect to Si-Ti rich alloys, make these intermetallic alloys less attractive for liquid assisted processes applied for densifying and joining techniques based on Si-Ti alloys. In addition, intermetallic phases and in particular silicides, do not “emerge” for their hardness and fracture

toughness values, in any case higher than pure Si [34]. On the contrary, silicides show improved thermo-mechanical properties and oxidation resistance at high temperatures [35]. Moreover, the decrease of process temperatures ($T \leq 1420°C$) and a better control of the microstructure evolution are easier achievable by moving the selection of infiltrating alloy to the Si-rich side of the Si-Ti phase diagram. For these reasons, liquid Si-Ti alloys seem a good compromise as infiltrants for C and SiC porous materials. However, in view to favour the Si-replacement the Si-Ti alloys selection must be carefully evaluated. Furthermore, aiming to the scale-up of the infiltration process up to the industrial level, several affecting factors should be deeply taken into account. Indeed, the starting metal materials may be not homogeneous and a Si-enrichment at the surface might be most probably favoured, as well as a $TiSi_2$ precipitation into the alloy bulk, during alloy manufacturing under not-well controlled atmospheres. Consequently, due to the presence of large amount of pure Si and silicides precipitates, anomalous melting can be observed. Moreover, the temperature selected during infiltration is usually around 1450°C, with a heating rate even slower than 5°C/min and the selected lower-melting Si-based alloys infiltrants may melt before reaching the imposed working temperature.

With such motivations behind, the influence of Si-content on the interaction phenomena taking place when a liquid Si-rich Si-Ti alloy is in contact with Glassy Carbon (GC) at T = 1450°C was investigated by the sessile drop method and the main relevant results are reported in the present work.

For the sake of clarity, the scope of the paper is to bring out the advantages of preliminary studies on wettability and interaction phenomena in optimizing the melt infiltration, mainly by addressing the selection of the most suitable set of operating parameters. In other words, by focusing on interfacial phenomena in terms of adhesion, reactivity, growth of reaction layers, etc., some factors negatively affecting the reactive infiltration process, (i.e. pore narrowing/pore closure and/or fibers-degradation by C-dissolution) can be easily predicted and limited to a large extent.

To check the reliability of the results obtained, the interfacial phenomena observed on GC substrates for two liquid Si-rich Si-Ti alloys, in terms of wetting kinetics and obtained interface microstructures, were compared with the experimental observations of wetting tests previously performed on liquid Si-rich Si-Ti eutectics (i.e. Si-16.4 at%Ti) in contact with GC [36] and Hot Pressed SiC [37] under the same operating conditions and by applying the same experimental procedures. Specifically, the Si-Ti hypereutectic (Si-24 at%Ti) and hypoeutectic (Si-8at%Ti) alloys were selected and put in contact with GC at T = 1450°C and the wetting kinetics analyzed in terms of contact angle values as a function of time, as well as the formed reaction products and developed interface microstructures.

Light Microscopy (LM) and Scanning Electron Microscopy (SEM), combined with an Energy Dispersive X-Ray Spectroscopy (EDS) were used to perform the interface microstructure characterization.

2. Wetting tests: experimental details

2.1 Materials and sample preparation

As substrate material for wetting experiments, Glassy Carbon (GC) was selected and used as provided by Alfa Aesar© and cut as plates (12 x 12 x 3 mm). At the GC substrate surface, the value of roughness Ra ≈ 20 nm was resulting by an optical confocal-interferometric profilometer (Sensofar S-neox) analysis.

The Si-Ti alloys were prepared by mixing and arc-melting nominal weights of high purity Si and Ti (99.98%-Goodfellow®). To ensure the homogeneity of their composition, the alloys were arc-melted more than 3 times under an Ar atmosphere (N60, $O_2 < 0.1$ ppm) while to decrease further the residual oxygen content inside the arc-melting chamber, a Zr drop was previously melted. By checking the alloys final weight as well as their actual composition by EDS analysis (Table 1), no evidence of loss of material by evaporation was observed.

The Si-8at% Ti and Si-24at% Ti alloys of 0.06 – 0.1 g were successfully obtained and the as-produced Si-Ti alloys microstructure and composition were inspected at the cross-sectioned samples by SEM/EDS, as shown in Figure 1.

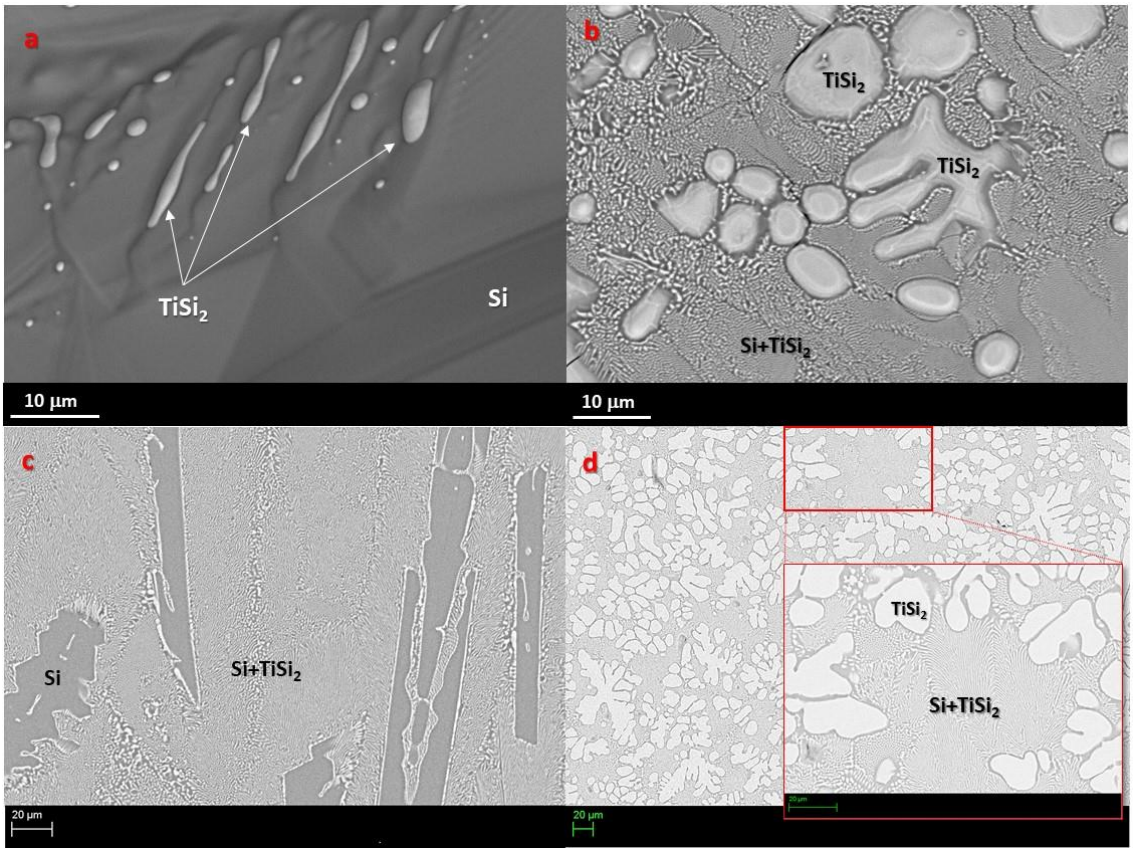

Figure 1. SEM-BSE images and phase identification by EDS analyses performed both at the (**a**) and (**b**) top of the solidified and at the (**c**) and (**d**) cross-sectioned Si-8at% Ti and Si-24at% Ti alloys samples after arc melting.

A strong Si-segregation was detected at the top of the Si-8at%Ti solidified drop (Figure 1a), as well as in the form of elongated needle-shaped crystals embedded into a Si-Ti eutectic phase at the cross-sectioned sample (Figure 1c). Contrarily, globular $TiSi_2$ crystals were observed at the top of Si-24 at% Ti solidified drop and even inside the alloy bulk as precipitates englobed in a Si rich Si-Ti eutectic microstructure. If compared with the Si-16.2 at% Ti alloy identified as the Si-rich Si-Ti eutectic alloy [30], such observations are in full agreement with hypo- and hyper- eutectics as it is the case for Si-24at%Ti and Si-8at%Ti, respectively [32].

Before the wetting experiments, both the alloy sample and the substrate were weighted, rinsed in an ultrasonic bath of isopropyl alcohol and dried with compressed air.

2.2 Sessile drop experiments: devices and procedures

The assembled at room temperature Si-Ti alloy/GC couple was inserted into the experimental device and moved to the central part of the heater.

Prior the experiments, the device was degassed under a vacuum ($P_{tot} \leq 10^{-6}$ mbar) for two hours. Wetting tests were carried out by the classical sessile drop method (SD) under a static Ar atmosphere (99.9999%, $O_2 < 0.1$ ppm) and by following the procedure detailed elsewhere [30]. It worth to highlight that the presence of graphite as heating element provides an atmosphere with reduced oxygen content ($PO_2 < 10^{-15}$ mbar), as reported in [30].

Wetting experiments were performed by raising the temperature up to the selected testing conditions (kept constant for 15 minutes) with a heating rate of 10°C/s. To preserve as much as possible the developed interface microstructures, the sample was "quenched" (cooling rate 20°C/s) at the end of the dwell time (15 minutes), by turning off the power to the heater.

The evolution of wetting kinetics, in terms of contact angle and drop geometric variables (R-base radius and H-drop height) values as a function of time, was in real-time followed and recorded by an image analysis software ad hoc-developed in LABVIEW environment (ASTRAVIEW® [38]) and connected to a high-speed CCD-camera.

To check the reliability of the results obtained, the experimental device described in detail in [39], was in parallel used to process and study the interaction phenomena occurring at the Si-24at%Ti/GC interface by capillary purification sessile drop method, even known as dispensed drop (DD), at T = 1450°C under a static Ar atmosphere [40].

At the testing temperature of T = 1450°C, the oxygen partial pressure value of $PO_2 < 10^{-14}$ mbar was achieved by the presence of Ta as heating element and acting as an oxygen getter [41]. Such methodology allows excluding possible affecting factors, mainly during the early stage of wetting, such as the presence of native oxide segregated at the alloy surface and delay in the melting due to a starting alloy with not homogenous microstructure. On the other hand, the absence of native oxide makes the molten surface directly in contact with the surrounding experimental environment, as well as with the tip of the capillary. Consequently, the molten phase is more prompt to evaporate or to be polluted by gas/liquid interactions and by reaction with the capillary.

The GC substrate and the Al_2O_3 capillary, filled by pieces of Si-24at%Ti alloy, were loaded into the device at room temperature. The experimental device was heated up to 800°C under a vacuum with a temperature gradient of 5°C/min. The second heating stage was performed under a static Ar atmosphere and the temperature was increased up to 1500°C for the complete melting of $TiSi_2$ precipitates [32]. Finally, the testing conditions were achieved by decreasing the temperature down to 1450°C, and then the molten alloy was squeezed and placed onto the GC substrate.

At the end of the isothermal time (t = 15 minutes), the device was cooled from T = 1450°C down to room temperature with a rate of 20°C/min.

Every single frame was processed by ASTRAVIEW® software and both contact angle values and drop geometric parameters measured to evaluate wettability and spreading behaviours over time. By analyzing the experimental methods/procedures applied and all the factors potentially affecting the reliability of the results, an accuracy of the contact angle data around ± 2° is estimated [42].

2.3. Surface and microstructural characterization

After the wetting tests, all the Si-Ti/GC samples were embedded in cold epoxy-resin, cross-sectioned, metallographically polished with SiC papers and diamond pastes, and coated with Au for microstructural characterization.

As already introduced, in order to analyze the microstructure and reaction products, both at the top and at the cross-sectioned solidified drops, a Light Microscopy (LM-ZEISS) and a Scanning Electron Microscope (SEM) equipped with Energy Dispersive X-Ray Spectroscopy detectors (EDS) were used.

3. Results

3.1 Wettability of GC by Si-rich Si-Ti alloys as a function of Si-content

In Figure 2, the evolution of contact angle values for the Si-8at%Ti/GC and Si-24at%Ti/GC systems are shown and compared with the wettability of GC by the liquid Si-16.2at%Ti eutectic alloy under the same operating conditions (i.e. T = 1450°C under a static Ar atmosphere [30]).

As it can be seen, the achievement of the steady state conditions seems influenced by the different Si-content (Figures 2a and 2b). Indeed, during the early stages of alloys spreading, the triple line of each Si-Ti/GC system exhibits a different kinetics behavior. In fact, the no-wetting to wetting transition was observed at 6, 10 and 18 s for Si-8at%Ti/GC, Si-16.2at%Ti/GC and Si-24at%Ti/GC couples, respectively, as evinced in Figure 2b and Figure 3. Moreover, after the first spreading stage, a decrease

in the slope of the wetting kinetics for all the couples was observed. Specifically, the decrease in the rate of spreading comes to be evident after 23, 27 and 30 sec after the detected Si-8at%Ti, Si-16.2at%Ti and Si-24at%Ti melting where the related contact angle values of θ ≈ 46°, 50° and 52° were measured. Subsequently, a further decrease of ≈ 2° in the contact angle value was observed for 7 seconds at the Si-8at%Ti/GC triple line. Contrarily, the achievement of the steady state conditions took longer time in the Si-24at%Ti/GC system, namely 60 seconds to exhibit a contact angle value of ≈ 46°, which was kept constant until the end of the dwell time (t = 900 s).

After a time of contact equal to t = 15 minutes between the liquid phase (Si-Ti alloys) and the solid substrate (GC) at T = 1450°C, the contact angle values measured were θ ≈ 41°, 44° and 46° for Si-8at%Ti/GC, Si-16.2at%Ti/GC and Si-24at%Ti/GC couples, respectively.

Figure 2c shows the triple lines of the three Si-rich Si-Ti alloys/GC samples after the wetting experiments. The "halo" surrounding the drop perimeters, markedly visible for the Si-richer systems, is attributed to the presence of a thin SiC layer, as detected by SEM/EDS analysis, similarly to other Si-rich based alloys processed under the same operating conditions [36, 37, 43-47], as shown in Figure 4.

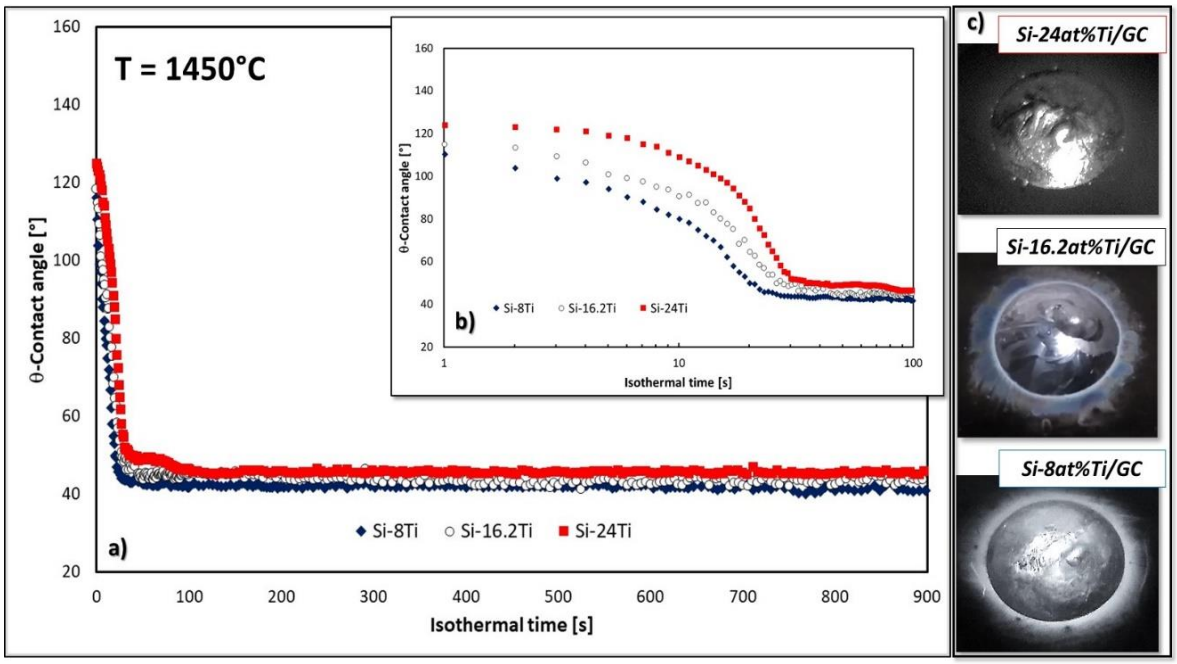

Figure 2. Contact angle behaviors observed at T = 1450 °C under an Ar atmosphere for (a) 900 s and (b) 100 s as a function of Si-content: (■) Si-24at%Ti /GC, (○) Si-16.28at%Ti/GC, (◆) Si-8at%Ti/GC and (c) and related top view photographs of Si-Ti alloys/GC couples after the wetting experiments.

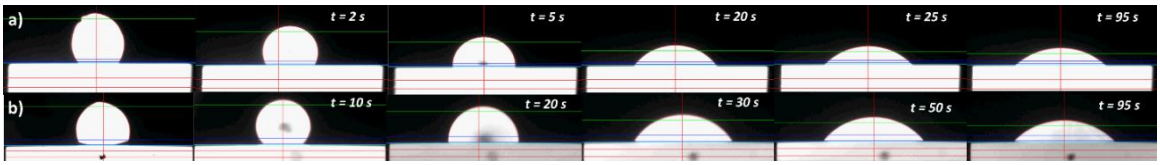

Figure 3. Time sequence images recorded during the wetting experiments performed by sessile drop method at T = 1450°C under an Ar atmosphere; (a) Si-8at%Ti/GC and (b) Si-24at%Ti/GC.

Specifically, a continuous SiC layer grown up on the GC surface was detected by SEM-BSE and EDS analyses in the Si-8at%Ti/GC system in a circular area surrounding the alloy drop for a distance around 20 μm. Conversely, moving far from the triple line, unreacted regions of GC appear with overlayered circular and narrowing areas of SiC. A less pronounced SiC layer was detected around the Si-24at%Ti alloy perimeter and even close to the Si-24at%Ti/GC triple line appearing as smaller crystals than those detected in the Si-8at%Ti/GC system (≈ 5 μm), as shown in the inserts of Figures

4a and 4b. Moreover, owing to the applied fast cooling of the two samples at the end of the wetting experiment, a crack at the interface was also observed in agreement with previous similar investigations.

A different alloy microstructure was found at the top of the solidified drops (Figures 4c and 4d). Specifically, three well distinguished developed microstructures were detected at the top of the Si-24at%Ti alloy and consisting in the Si+$TiSi_2$ eutectic phase and elongated crystals of pure Si embedded in a two-phase of Si + colonies of segregated micro crystals of $TiSi_2$ (Figure 4c). Contrarily, at the top of the solidified Si-8at%Ti/GC couple, except a few "rejected" micro crystals of $TiSi_2$ at the grain boundaries of the eutectic phase, the latter microstructure was not revealed by SEM-BSE and EDS analyses (Figure 4d). On the other hand, elongated crystals of pure Si were found segregated at the alloy surface, as expected.

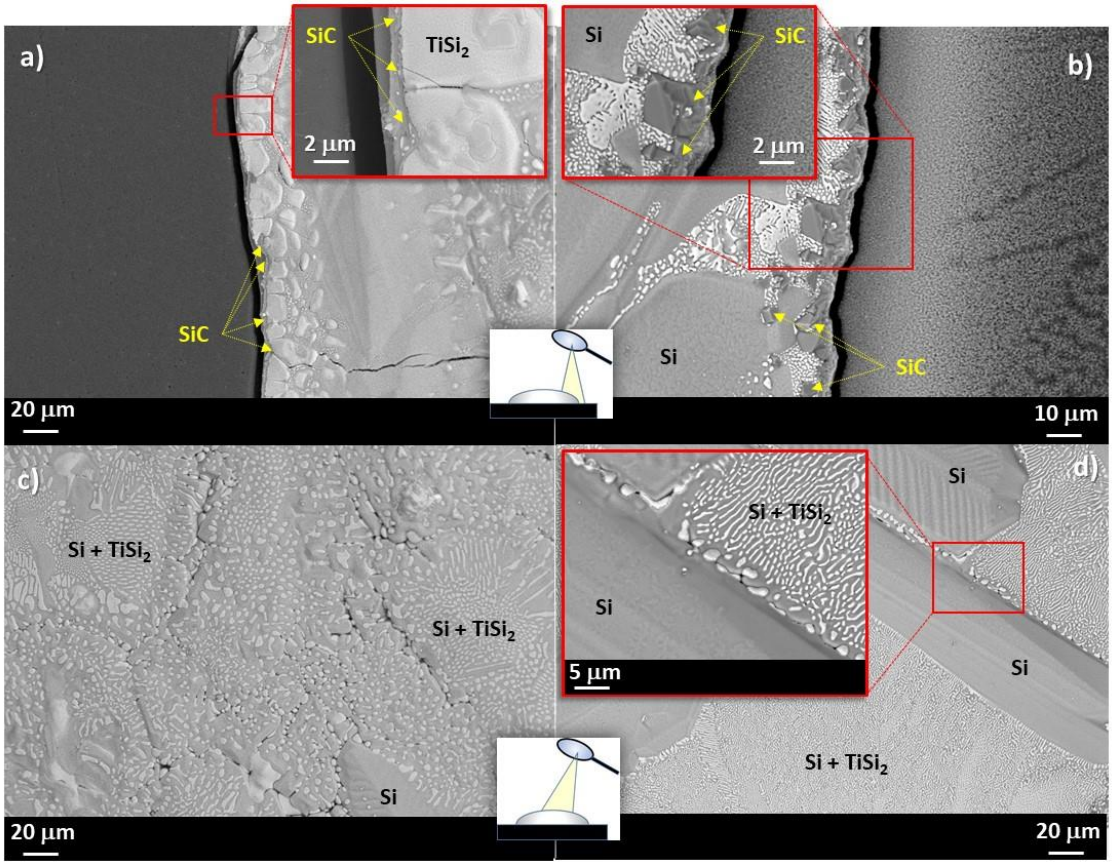

Figure 4. SEM-BSE images and proposed phase identification by EDS analyses performed at different magnifications at the triple lines and at top of the (**a**), (**c**) Si-24at%Ti/GC and (**b**), (**d**) Si-8at%Ti/GC samples after the wetting tests performed at T = 1450 °C for 15 min.

The less pronounced growth of SiC crystals at the Si-24at%Ti/GC interface respect to the Si-8at%Ti/GC is confirmed also by BSE-EDS analyses performed at the the cross-sectioned sample after the wetting test, as shown in Figure 5. As it can be seen, a compact layer of SiC with a thickness less than 2 µm is detected (Figure 5a). Moving toward the middle of the drop, a different microstructure was observed and resulting in a thicker layer of SiC consisting in a first continuous plane (< 2 µm), similar to the layer observed at the triple line, with stacked over SiC crystals epitaxially grown up to 5-7 µm, as shown in Figure 5c. In the case of the Si-24at%Ti/GC solidified sample, a Si-$TiSi_2$ two-phase microstructure consisting in globules-shaped $TiSi_2$ crystals embedded in a Si matrix was observed in the alloy drop after solidification. In particular, an increase of $TiSi_2$ crystals size was revealed moving from the middle of the drop (Figure 5c) to the triple line (Figure 5a). A comparable SiC layer was detected at the Si-8at%Ti/GC interface in terms of size and microstructure, as shown in Figure 5d. Although the SiC layer average thickness is comparable with Si-24at%Ti/GC sample, at the Si-8at%Ti/GC triple line, a more compact layer is observed as the result of an enhanced SiC-crystals

packaging phenomenon (Figure 5b). Contrarily, the alloy microstructure at the metal-ceramic interface totally differs respect to the Si-24at%Ti/GC couple. In fact, in the Si-8at%Ti/GC sample, a two-phase system is found after the solidification resulting in pure Si crystals surrounded by the Si+$TiSi_2$ eutectic phase (Figures 5b and 5d).

Figure 5. SEM-BSE images and proposed phase identification by EDS analyses performed at different magnifications at the triple lines and at the interfaces of the cross-sectioned (a), (c) Si-24at%Ti/GC and (b), (d) Si-8at%Ti/GC samples after the wetting tests performed at T = 1450 °C for 15 min.

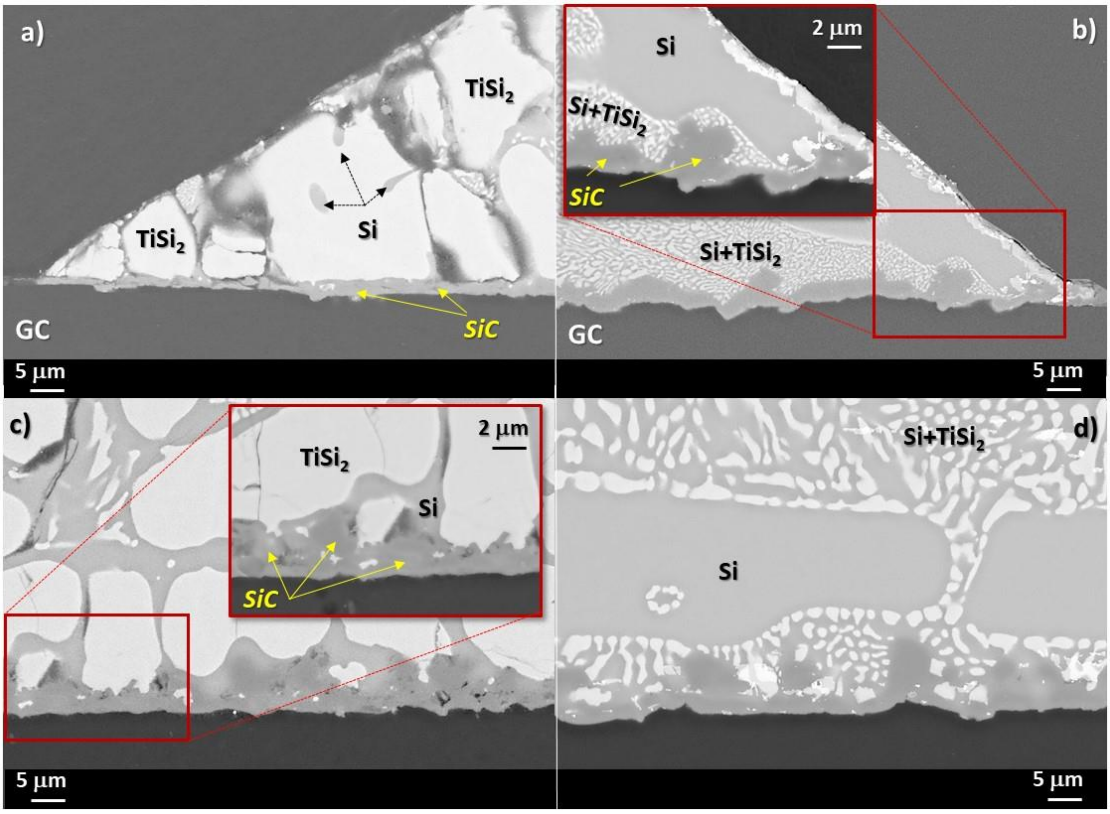

3.2 Wettability of GC by Si-24at%Ti alloys as a function of the testing method

As aforementioned, to check the reliability of the results obtained, as well as to investigate affecting factors on the spreading kinetics, such as not homogeneous starting materials and the presence of pollutants, a targeted wetting experiment was performed at T = 1450°C by dispensing a liquid Si-24at%Ti alloy through an Al_2O_3 capillary onto the GC plate.

Aiming to achieve the complete alloy homogenization by melting $TiSi_2$ precipitates (Figure 1d), the metal material inside the capillary was overheating up to 1500°C for a few minutes, then the testing temperature of T = 1450°C was imposed and the alloy squeezed on the GC plate. Figure 6 shows the time sequence of the more relevant images recorded during the alloy squeezing from the capillary (1-4), the melt deposition on the GC substrate (5-7) and the wetting test (8-11). Although the image recording rate was 10 frames/s, just after the alloy detachment from the capillary, a contact angle value of $\theta \approx 37°$ was shown at the newly formed Si-24at%Ti/GC interface and the mentioned value was kept constant until the end of the experiment (t = 15 min), as shown in Figure 6. Similarly to the sample processed by classical sessile drop method, three well distinguished developed microstructures were detected at the top of the Si-24at%Ti/GC solidified couple (Figure 7b) and consisting of a Si-$TiSi_2$ two-phase microstructure embedded in a Si matrix, plus globules-shaped $TiSi_2$ crystals segregated at the alloy surface.

Beyond the triple line, residual amounts of alloy (Figures 7a and 7c), as well as a thin layer of nanometric SiC crystals, were detected on the GC substrate. A well-compacted layer of nanometric SiC crystals was also detected at the triple line (Figures 7d and 7e), as well as overlayered colonies of SiC crystals epitaxially grown up to a size of 2-7 µm.

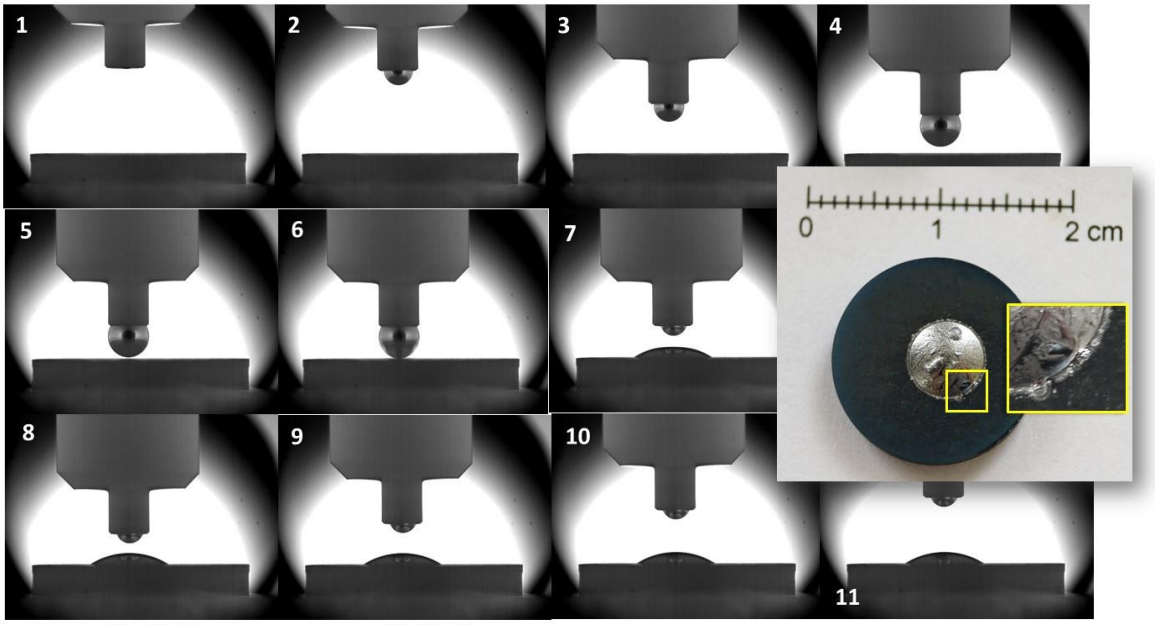

Figure 6. Post-mortem picture of the Si-24at%Ti/GC sample and the time sequence of images recorded during the wetting test performed by the dispensed drop method at T =1450°C under an Ar atmosphere.

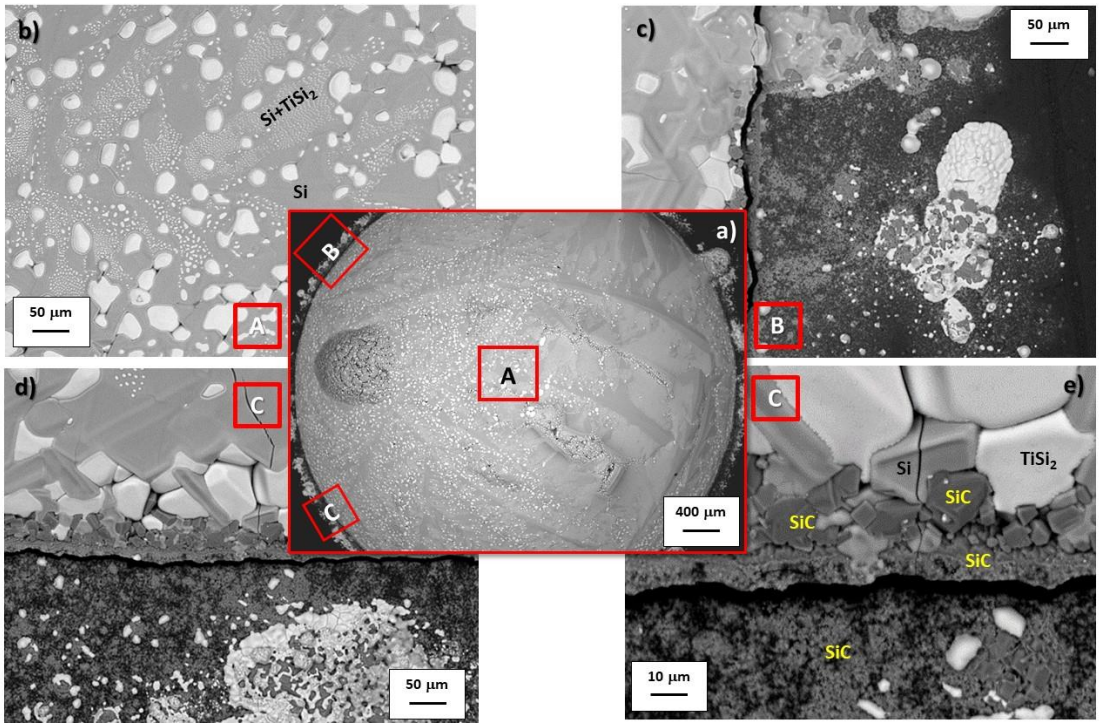

Figure 7. SEM-BSE and phase identification by EDS analyses performed at different magnifications at the top (a), (b) and at the triple line (c), (d) and (e) of the solidified Si-24at%Ti/GC sample after the wetting test performed by the dispensed drop method at T =1450 °C under an Ar atmosphere.

At the Si-24at%Ti/GC interfaces obtained by the two different methods, mostly the same developed microstructure was observed (Figures 8a and 8b). In both cases, globular-shaped $TiSi_2$ crystals were observed in the alloy (closely to the alloy/GC interface line) as "embedded" in pure Si and in a Si-rich Si-Ti eutectic phase moving forward to the top of the alloy drop.

Similarly to the sample obtained by classical sessile drop method, also in this case a SiC layer was detected as the unique reaction product at the center of the interface (Figure 8d). In particular, a 2 µm

SiC compact layer covered by SiC epitaxial crystals (size 2-7 µm) was again found. The same microstructure was noticed at the triple line of the Si-24at%Ti/GC sample (Figure 8c).

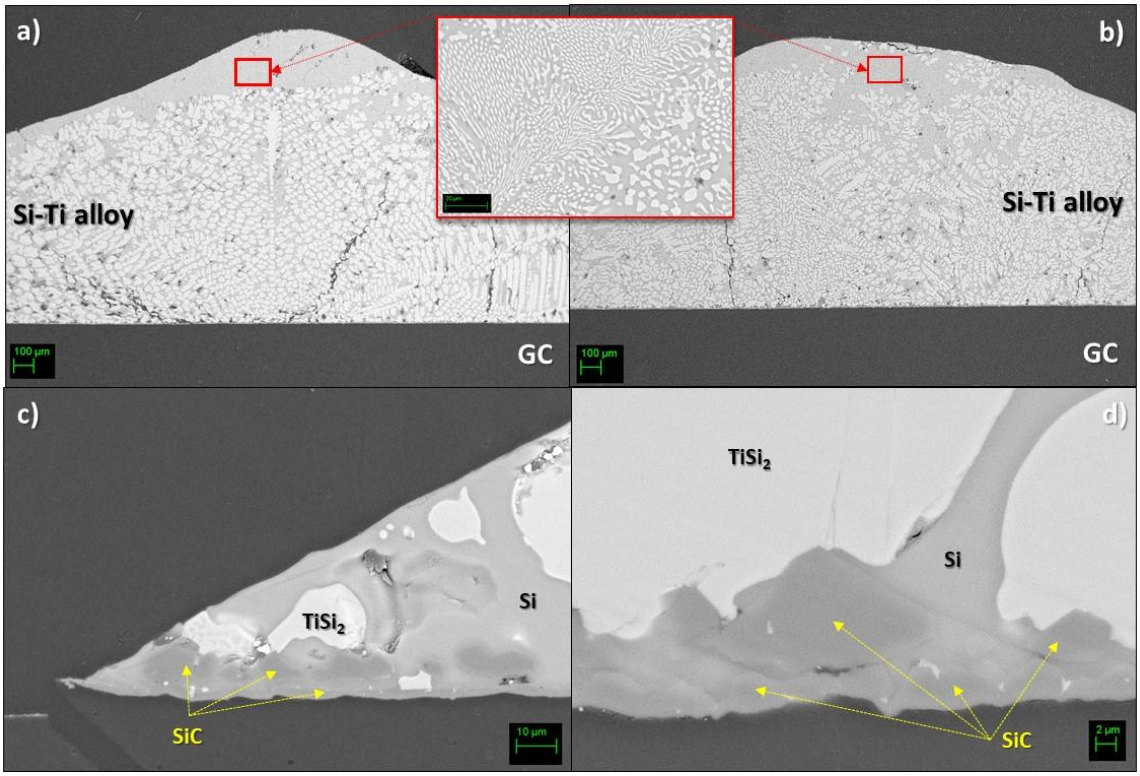

Figure 8. SEM-BSE images and phase identification by EDS analyses performed at different magnifications at the cross-sectioned Si-24at%Ti/GC samples processed by (a) classical sessile and (b), (c), (d) dispensed drop methods at T =1450°C under an Ar atmosphere.

4. Discussion

As introduced, the paper aims to study the feasibility of using Si rich Si-Ti alloys for favouring infiltration process in the manufacture of SiC/$TiSi_2$ composites. In addition to their low weight, such advanced materials are known for their high oxidation/corrosion resistances.

A very good wetting (i.e $\theta << 90°$) between the infiltrating alloy and the porous material is one of the key requirements making spontaneous melt infiltration as a successful process for the cost-less fabrication of nearly net-shaped composites.

Accordingly, as evinced by the results presented in this work on the wettability of GC by liquid Si rich Si-Ti alloys at T = 1450°C under an Ar atmosphere, the alloys investigated are excellent candidates as infiltrating metal materials for C- and SiC-based porous systems to fabricate SiC/$TiSi_2$ composites by RFSC process. Indeed, a very good wetting was shown at the Si-Ti alloys/GC triple lines, as detailed in the Table 1. In addition, for all the systems investigated, SiC was detected as the unique reaction product (Figures 5 and 8), which is in agreement with the minimun content of Si (X^{Si}_{eq}) in the alloy enabling spontaneous infiltration mechanism controlled by reactivity. Specifically, the X^{Si}_{eq} is the composition for which all phases involved (Si–Ti/SiC/C) are in equilibrium. The value of X^{Si}_{eq} can be predicted by using thermodynamic calculations [48], and it is a key parameter for selecting the suitable range of Si-based alloy compositions to succed in the fabrication of composites by reactive infiltration process. On the other hand, as infiltration proceeds, the alloy composition may shift towards a composition richer in the alloying element (Me), which might affect the infiltration kinetics due to the reduced reactivity, or to the appearance of unexpected competitive reactions between the Si alloying element and the C-based porous material, as following:

$$Me + C \rightarrow Silicide + Carbide \quad (1)$$

Table 1. Equilibrium contact angle values (θ_f) measured for the liquid Si-rich Si-Ti alloys in contact with GC and SiC at T = 1450°C under an Ar atmosphere by the sessile drop (SD) and dispensed drop (DD) methods.

System	Method	T [°C]	t [min]	$\theta_f \pm 2$ [°]	Reference
Si/GC	SD	1450	15	38	[47]
Si-8at%Ti/GC	SD			42	This work
Si-16at%Ti/GC	SD			43	[36, 37]
Si-24at%Ti/GC	SD			46	This work
Si-16at%Ti/GC	DD			41	[36]
Si-24at%Ti/GC	DD			37	This work
Si-16at%Ti/SiC	SD			44	[37]

A X^{Si}_{eq} value of 0.69 was calculated for Si-Ti/SiC/C system at T = 1450°C which is approaching to the Si-content of the $TiSi_2$ alloy ($X^{Si} = 0.66$). Similar confirmation can be obtained by analysing the recent studies reported by Roger et al. on Si-Ti-C [27, 28] based on thermodynamic calculations using Thermo-Calc software [49] and the thermodynamic description reported by Y. Du et al. [50]. As it can be seen from the ternary phase diagram calculated for Si-Ti-C system at T = 1450°C, bifase equilibria are predicted for a Si content less than 66 at% in the Si-Ti alloy compositions. Namely, for Si-Ti alloys with a Si content < 0.66, the coexistance of Si, $TiSi_2$ and SiC is predicted, as confirmed by the results here presented.

After 15 minutes, the contact angle values shown at the Si-Ti alloys/GC triple lines at T = 1450°C are almost comparable and in agreement with other similar Si-rich systems previously investigated [24-26, 30, 36, 37, 43-47]. On the other hand, a general trend of decreasing in the final contact angle measured after 15 minutes with the increasing of Si content is noticed. However, taking into account the experimental error, such tendency is less pronounced in the composition range from eutectics to pure Si and the final contact angle is almost coincident, as reported in Table 1. Contrarily, if the wetting kinetics (U_{wett}) is analysed, it results that U_{wett} (Si-24at%Ti) < U_{wett} (Si-16.2at%Ti) < U_{wett} (Si-8at%Ti). Such outcomes seem in contradiction with similar results reported in the literature [44] where a weak decrease in the spreading kinetics was observed with the increase of Si content in the Si-Co system processed under the same experimental conditions. As a general consideration, the increase of Si should increase the Si-based alloy reactivity towards GC resulting in stronger C-dissolution and reactivity. Indeed, after 60 minutes, a thicker layer of SiC was observed at the Si-Co alloy richer in Si. On the other hand, as documented in [45, 51], the growth and thickening of SiC at the interface are time-dependent phenomena and more evident after 15 minutes.

As known, the early stage of spreading occurring during classical sessile drop wetting experiments may be affected by the melting stage, which in turn can be influenced by the presence of a) a primary oxide layer (SiO_2) at the alloy surface, which is dissolved in Si monoxide by the reaction with Si [36], as well as by b) a non-homogenous starting composition of the melting phase. After all, the presence of the detected higher melting $TiSi_2$ precipitates (Tm = 1485°C [32]) dispersed in the eutectic phase for Si-16.2at%Ti [37] and Si-24at%Ti (Figure 1) may be the determing factor for the delay observed in achieving the complete alloy melting (Figure 3) and, consequently even influencing the alloy spreading kinetics onto the GC substrate, as well as in the early stage interaction phenomena taking place at the Si-Ti alloys/GC interfaces.

As it can be seen in Figure 4, and in agreement with previous results obtained by processing Si-16.2at%Ti/GC system under the same experimental conditions, strong Si-evaporation / condensation phenomena were observed, mainly in the Si-8at%Ti/GC sample. Although processed at the same temperature, the less pronounced Si-evaporation resulting in the presence of a thin layer

of SiC beyond the triple line, observed in the Si-24at%Ti/GC couple, may be explained by difficulties encountered to achieve the steady state conditions at the interface. In addition, the absence of individual epithaxially grown SiC crystals was noticed at the triple line of the cross-sectioned Si-24at%Ti/GC sample (Figure 5). Contrarily, the usual developed microstructure of the reaction product consisting in a first layer of SiC with above well distinguishable SiC crystals was found at the interface close to the middle of the drop. Such experimental observations let us to conclude that during the early stage of spreading, owing to the delay in achieving the complete melting and in crossing the transition limit between no-wetting to wetting behaviour, strong interfacial phenomena were already taking place. The absence of SiC crystals at the triple line may be due to the Si consumption during the alloy spreading. As a consequence, the reduced Si content at the triple line respect to the interface located at the central part of the Si-24at%Ti/GC sample, might have affecting diffusion phenomena between the alloy and the substrate. The poor Si content at the triple line may be even the reason for the higher contact angle value measured at the triple line at the end of the wetting test, as well as the precipitation of $TiSi_2$ globular crystals during the solidification with a size bigger than those observed in the central part of the Si-24at%Ti/GC couple. Contrarily, a Si+TiSi2 two-phase was observed in the Si-24at%Ti alloy in contact with GC both at the triple line and moving to the central part of the sample, after wetting test performed by the dispensed drop method under the same experimental conditions (Figure 8). However, as it can be seen in Figures 6 and 7, the presence of residual amount of alloy material on GC close to the triple line put in evindence a dewetting phenomenon most probably occurred after the alloy deposition onto the GC substrate. It is caused by the alloy perturbation when it is placed onto a substrate and subsequently detachement by moving up the capillary [37]. On the other hand, dewetting is mainly observed at the interface of negligible or less reactive systems. The less reactivity of the liquid Si-24at%Ti alloy respect to GC could be explained by the presence of a not continuous thin layer of SiC already appeared during the approaching of the pendant drop to the substrate, which is responsible for the decreasing of the contact angle value at the triple line (Table 1), as observed in [46]. Indeed, a well adherent GC/SiC/Si-based alloy system is observed at the end of wetting tests. The strong adherence is responsible for the crack at the interface together with the mismatch in the GC/SiC/Si-Silicides CTE values.

5. Conclusions

To succeed in the fabrication of $SiC/TiSi_2$ lightweight composites by reactive infiltration, the feasibility of using Si rich Si-Ti alloys as infiltrating alloys was studied. In particular, the Si-Ti alloys investigated seem excellent candidates as infiltrating metal materials for C- and SiC-based porous systems to fabricate $SiC/TiSi_2$ composites by RFSC process.

Specifically, based on to the results obtained by wetting experiments at Si-Ti alloys/GC interfaces performed at T = 1450°C under an Ar atmosphere by the classical sessile drop methods, the Si-rich Si-Ti alloys selected meet the key requirements for evolving reactive infiltration by spontaneous mechanism. Indeed, a very good wetting was observed at the triple lines (i.e $\theta << 90°$) where comparable contact angle values were measured after 15 minutes. On the other hand, Si-content seems weakly affecting the spreading kinetics mainly due to not homogeneous starting alloy materials. Such conclusion is substantiated by the results obtained during experiments performed by squeezing the alloy through the capillary. The absence of primary oxide at the alloy surface, as well as an improved homogenization, were crucial for obtaining a regular Si-24at%Ti/GC interface. Namely, in fully agreement with thermodynamics and similar studies reported in literature, it was consisting of a compact layer of SiC detected as unique reaction product, with overgrown up epitaxial SiC-crystals with a size ranging from 2 μm to 7 μm.

In this regard, the compactness of the reaction layer is favoured by the increase of Si-content in the alloy composition, as well as are the Si-condensation/evaporation phenomena observed beyond the advancing triple line and the presence of elongated Si crystals inside the alloy, most probably grownduring the sample solidification. Mainly for the latter reason, for preserving the overall

thermo-mechanical response of the produced composite a Si content larger than the eutectic composition is not suggested.

Author Contributions: All authors have read and agree to the published version of the manuscript. Conceptualization, D.G., S. G; S.D., R.N.; methodology, D.G., G.B., R.N., W.P.; validation, D.G., S.G., R.N.; formal analysis, D.G. S.G., S.D., R.N.; investigation, D.G, R.N.; writing—original draft preparation, D.G., S.G; writing—review and editing, D.G., R.N.; supervision, D.G., N.S; Funding resources D.G., N.S.

Acknowledgments:
The work performed at CNR-ICMATE (Italy) and KIT-Krakow (Poland) was supported by National Science Center of Poland through POLONEZ project number UMO-2016/23/P/ST8/01916. This project was carried out under POLONEZ-3 program which has received funding from European Union's Horizon 2020 research and innovation program under Marie Skłodowska-Curie grant agreement. No 665778.

DG wishes to thank Mr. Francesco Mocellin for technical assistance on the expeerimental devices.

Conflicts of Interest: The authors declare no conflict of interest.

References

[1] B.D. Dunn, Materials and Processes for Spacecraft and High Reliability Applications, Springer International Publishing Switzerland 2016.
[2] D.B. Miracle, Aeronautical applications of metal-matrix composites. In: Henry, S.D., et al. (Eds.), ASM Handbook. ASM International, Ohio, USA, 2001.
[3] H. Singh, S.J. Nrip, A.K. Tyagi, An overview of metal matrix composite: Processing and SiC based mechanical properties, Journal of Engineering Research and Studies, 2 (4) (2011) 72-78.
[4] E.P. Simonenko, D.V. Sevastyanov, N.P. Simonenko, V.G. Sevastyanov, N.T. Kuznetsov, Promising Ultra_High_Temperature Ceramic Materials for Aerospace Applications, Russian Journal of Inorganic Chemistry, 58 (14)(2013) 1669–1693.
[5] D.B. Miracle, High entropy alloys as a bold step forward in alloy development, Nature Communications 10 (1) (2019) 1805
[6] D.C. Hofmann, S.N. Roberts, Microgravity metal processing: from undercooled liquids to bulk metallic glasses, Nature Communications 1 (2015) 15003.
[7] Timo Nieberle, Shiv Ranjan Kumar, Amar Patnaik, and Chandramani Goswami, Review: Composite Materials for Armour Application, In: Rakesh P.K., Sharma A.K., Singh I. (eds) Advances in Engineering Design. Lecture Notes in Mechanical Engineering. Springer, Singapore. https://doi.org/10.1007/978-981-33-4018-3_22
[8] J. Binner, M. Porter, B. Baker, J. Zou, V. Venkatachalam, V. R. Diaz, A. D'Angio, P. Ramanujam, T. Zhang, T. S. R. C. Murthy, Selection, processing, properties and applications of ultra-high temperature ceramic matrix composites, UHTCMCs – a review, (2019) International Materials Reviews, DOI: 10.1080/09506608.2019.1652006.
[9] S.T. Mileiko, Constituent Compatibility and Microstructural Stability, Comprehensive Composite Materials, 4 (2000) 265-287.
[10] G. Liu, X. Zhang, J. Yang, G. Qiao, Recent advances in joining of SiC-based materials (monolithic SiC and SiCf/SiC composites): Joining processes, joint strength, and interfacial behavior, Journal of Advanced Ceramics, 8 (1) (2019) 19–38.
[11] X. Wua, B. Peia, Y. Zhua, Z. Huanga, Joining of the C_f/SiC composites by a one-step Si infiltration reaction bonding, Materials Characterization 155 (2019) 109799.
[12] F. Lamouroux, S. Bertrand, R. Pailler, R. Naslain, M. Cataldi, Oxidation-resistant carbon-fiber-reinforced ceramic-matrix composites, Compos. Sci. Technol. 59 (1999) 1073-1085.
[13] H. Hald, Operational limits for reusable space transportation systems due to physical boundaries of C/SiC materials, Aerosp. Sci. Technol., 7 (2003) 551-559.

[14] LY. Wang, R.Y. Luo, G.Y. Cui, Z.F. Chen, Effects of pyrolysis temperatures on the oxidation behavior of PIP-processed SiCf/SiC composites, Ceramics International 46 (2020) 17846–17847.
[15] G. Pulci, M. Tului, J. Tirillo, F. Marra, S. Lionetti, T. Valente, High Temperature Mechanical Behavior of UHTC Coatings for Thermal Protection of Re-Entry Vehicles, Journal of Thermal Spray Technology, 20 (1-2) (2011) 139-144.
[16] V. Casalegno, S. De La Pierre Deambrosis, I. Corrazzari, F. Turci, P. Tatarko, O. Damiano, L. Cornillon, A. Terenzi, M. Puglia, L. Torre, M. Ferraris, Design, Realization, and Characterization of Advanced Adhesives for Joining Ultra-Stable C/C Based Components, Macromolecular Materials and Engineering 305 (9) (2020) 2000229.
[17] T. Koyanagi, Y. Katoh, T. Hinoki, C. Henager, M. Ferraris, S. Grasso, Progress in development of SiC-based joints resistant to neutron irradiation, Journal of the European Ceramic Society 40 (4) (2020) 1023-1034.
[18] M. Li, X. Zhou, H. Yang, S. Du, Q. Huang, The critical issues of SiC materials for future nuclear systems, Scripta Mater. 143 (2018) 149-153.
[19] M. Salvo, P. Lemoine, M. Ferraris, M. Montorsi, Joining of carbon-carbon composites for thermonuclear fusion applications, J. Am. Ceram. Soc. 80 (1) (1997) 206-212.
[20] J.N. Ness and T.F. Page, Microstructural Evolution in Reaction-Bonded Silicon Carbide, J. Mater. Sci. 21(1986) 1377–1397.
[21] A.J. Whitehead and T.F. Page, Fabrication and Characterization of Some Novel Reaction-Bonded Silicon Carbide Materials, J. Mater. Sci. 27 (1992) 839–852
[22] E. Jacques, Y. Le Petitcorps, L. Maillé, C. Lorrette, L. Chaffron, Joining Silicon Carbide plates by Titanium, Powder Metallurgy and Metal Ceramics, 52 (9-10) (2014) 606-611.
[23] Z. He, C. Li, J. Qi., Y. Huang, J. Feng, J. Cao, Pre-infiltration and brazing behaviors of Cf/C composites with high temperature Ti-Si eutectic alloy, Carbon 140 (2018) 57-67.
[24] B. Riccardi, C.A. Nannetti, J. Woltersdorf, E. Pippel, T. Petrisor, Joining of SiC based ceramics and composites with Si-16Ti and Si-18Cr eutectic alloys, Int. J. Materials and Product Technology, 20 (5-6) (2004) 440-451.
[25] Z. He, C. Li, X. Si, J. Qi, J. Cao, Wetting of Si–14Ti alloy on SiC_f/SiC and C/C composites and their brazed joint at high temperatures, Ceramics International 47 (10) (2021) 13845-13852.
[26] Z. He, C. Li, B. Lan, C. Zhang, J. Qi, Y. Huang, J. Feng, J. Cao, *In situ* $TiSi_2$ microarray reinforced Si–Ti eutectic colonies in C_f/C composite joints for high-temperature application, Ceramics International 46 (8) (2020) 10495-10502.
[27] J. Roger, M. Salles, Kinetics of liquid metal infiltration in TiC-SiC or SiC porous compacts, Journal of Alloys and Compounds 860 (2021) 158453.
[28] J. Roger, M. Salles, Thermodynamic of liquid metal infiltration in TiC–SiC or SiC porous compacts, Journal of Alloys and Compounds 802 (2019) 636-648.
[29] L. Maillé, S. Le Ber, M.A. Dourges, R. Pailler, A. Guette, J. Roger, Manufacturing of ceramic matrix composite using a hybrid process combining $TiSi_2$ active filler infiltration and preceramic impregnation and pyrolysis, Journal of the European Ceramic Society 34 (2) (2014) 189-195.
[30] D. Giuranno, N. Sobczak, G. Bruzda, R. Nowak, W. Polkowski, A. Polkowska, A. Kudyba, R. Novakovic, Studies of the Joining-Relevant Interfacial Properties in the Si-Ti/C and Si-Ti/SiC Systems, Journal of Materials Engineering and Performance 29 (2020) 4864-4871.
[31] P. Dadras, T.T. Ngai, G.M. Mehrotra, Joining of carbon-carbon composites using boron and titanium disilicide interlayers, J. Am. Ceram. Soc. 80 (1) (1997) 125-132.
[32] T.B. Massalski, Binary Alloy Phase Diagrams, Vol 1,2, ASM, Metals Park, 1986.
[33] T. Iida and R. I. L. Guthrie, The Physical Properties of Liquid Metals, Clarendon Press, Oxford, 1993.
[34] D. Moskovskikh, S. Vorotilo, V. Buinevich, A. Sedegov, K. Kuskov, A. Khort, C. Shuck, M. Zhukovskyi, A. Mukasyan, Extremely hard and tough high entropy nitride ceramics, Scientific Reports 10 (2020) 19874.
[35] R. Mitra, Mechanical Behavior and Oxidation Resistance of Structural Silicides, International Materials Reviews 51 (1) (2006)13-64.
[36] D. Giuranno, N. Sobczak, G. Bruzda, R. Nowak, W. Polkowski, A. Kudyba, A. Polkowska, R. Novakovic, Studying the Wettability and Reactivity of Liquid Si-Ti Eutectic Alloy on Glassy Carbon, Journal of Materials Engineering and Performance, 28 (2019) 3460-3467.
[37] D. Giuranno, N. Sobczak, G. Bruzda, R. Nowak, W. Polkowski, A. Kudyba, A. Polkowska, R. Novakovic, Wetting and spreading behaviors of liquid Si-Ti eutectic alloy in contact with glassy carbon and SiC at T = 1450°C, Metall and Mat. Trans. A, 50 (10) (2019) 4814-4826.
[38] L. Liggieri, A. Passerone, An automatic technique for measuring the surface tension of liquid metals, High. Technol. 7 (1989) 80-86.

[39] N. Sobczak, R. Nowak, W. Radziwill, J. Budzioch, A. Glenz, Experimental complex for investigations of high temperature capillarity phenomena, Mat. Sci. Eng. A 495 (2008) 43–49.
[40] E. Ricci, D. Giuranno, N. Sobczak, Further development of testing procedures for high temperature surface tension measurements, Journal of Materials Engineering and Performance 22 (11) (2013) 3381-3388.
[41] O. Knacke, O. Kubashewski, K. Hesselmann, Thermochemical Properties of Inorganic Substances, 2nd ed., Springer Verlag, Düsseldorf, 1991.
[42] N. Eustathopoulos, N. Sobczak, A. Passerone, K. Nogi, Measurement of contact angle and work of adhesion at high temperature, J. Mat. Sci., 2005, 40, 2271-2280.
[43] B. Drevet, N. Eustathopoulos, Wetting of ceramics by molten silicon and silicon alloys: a review, J. Mat. Sci., 47 (2012) 8247–8260.
[44] M. Caccia, S. Amore, D. Giuranno, R. Novakovic, E. Ricci, J. Narciso. Towards optimization of SiC/$CoSi_2$ composite material manufacture via reactive infiltration: Wetting study of Si–Co alloys on carbon materials. Journal of the European Ceramic Society 35 (15) (2015) 4099-4106.
[45] D. Giuranno, A. Polkowska, W. Polkowski, R. Novakovic, Wetting behavior and reactivity of liquid Si-10Zr alloy in contact with glassy carbon, J. Alloys Compd., 822 (2020) 153643.
[46] D. Giuranno, G. Bruzda, A. Polkowska, R. Nowak, W. Polkowski, A. Kudyba, N. Sobczak, F. Mocellin, R. Novakovic, Journal of the European Ceramic Society, Design of refractory SiC/ZrSi2 composites: Wettability and spreading behavior of liquid Si-10Zr alloy in contact with SiC at high temperatures 40 (4) (2020) 953-960.
[47] D. Giuranno, W. Polkowski, G. Bruzda, A. Kudyba, J. Narciso, Interfacial Phenomena between Liquid Si-rich Si-Zr Alloys and Glassy Carbon, Materials MDPI 13 (5) (2020) 1194- .
[48] N. Eustathopoulos M.G. Nicholas B. Drevet, Wettability at High Temperatures, Volume 3, Pergamon 1999.
[49] J.O. Andersson, T. Helander, L. Höglund, P.F. Shi, B. Sundman, Thermo-Calc and DICTRA, computational tools for materials science, Calphad, 26 (2002), 273-312
[50] Y. Du, J.C. Schuster, H.J. Seifert, F. Aldinger, Experimental investigation and thermodynamic calculation of the titanium–silicon–carbon system, J. Am. Ceram. Soc., 83 (2000) 197-203.
[51] R. Voytovych, R. Israel, N. Calderon, F. Hodaj, N. Eustathopoulos, Reactivity between liquid Si or Si alloys and graphite, J. Eur. Ceram. Soc. 32 (14) (2012) 3825e3835.